ISSN 1590-2595

quaderni di geofisica

n. 51

SEISMIC NOISE AT SOLFATARA VOLCANO (CAMPI FLEGREI, ITALY): ACQUISITION TECHNIQUES AND FIRST RESULTS

Simona Petrosino et alii

Istituto Nazionale di Geofisica e Vulcanologia

2008

Segreteria di Redazione
Francesca Di Stefano (responsabile)
Tel. +39 06 51860068
Fax +39 06 36915617
Rossella Celi
Tel. +39 06 51860055
Fax +39 06 36915617
redazionecen@ingv.it

quaderni di geofisica

SEISMIC NOISE AT SOLFATARA VOLCANO (CAMPI FLEGREI, ITALY): ACQUISITION TECHNIQUES AND FIRST RESULTS

RUMORE SISMICO AL VULCANO SOLFATARA (CAMPI FLEGREI): TECNICHE DI ACQUISIZIONE E PRIMI RISULTATI

Simona Petrosino[1], Norma Damiano[2], Paola Cusano[1], Mariacira Veneruso[2], Lucia Zaccarelli[1], Vincenzo Torello[1], Edoardo Del Pezzo[1]

[1]Istituto Nazionale di Geofisica e Vulcanologia, Sezione di Napoli - Osservatorio Vesuviano

[2]Centro Regionale di Competenza "Analisi e Monitoraggio del Rischio Ambientale" (AMRA)

Indice

Abstract

In the period 2-6 April 2007 a seismic survey was carried out at Solfatara Volcano, with the aim of inferring the shallow structure and evaluating local site effects. Seismic noise was recorded by five circular seismic arrays deployed in different areas of the crater. The geometry was designed in order to obtain also a sub-configuration consisting of two profiles oriented in the N-S and E-W directions. An other seismic station was installed on the eastern rim of the crater, for a hardrock reference. A preliminary spectral analysis was performed on some samples of seismic noise recorded during the experiment.

As future development, surface wave dispersion will be obtained by using array techniques, such as the Spatial Autocorrelation method (SPAC) of Aki (1957) and its recent modifications (MSPAC, Bettig et al, 2001; CCA, Cho et al., 2004). The shear-wave velocity models will be inferred for each array from the inversion of the dispersion curves. Moreover experimental site transfer functions will be evaluated for each station, using both Nakamura's technique and the reference-site spectral ratio method.

The high density of the deployment and the large number of the sampled sites will allow to obtain a detailed shallow velocity structure and to map resonance frequencies and amplification values in different areas of the crater.

Riassunto

Dal 2 al 6 Aprile 2007 si è svolta una campagna di acquisizione di dati sismici al vulcano Solfatara, con lo scopo di determinare la struttura crostale superficiale e valutare gli effetti di sito locali. Il rumore sismico è stato registrato utilizzando cinque array circolari installati in differenti aree del cratere. La configurazione degli array è stata realizzata in modo tale che alcuni sensori fossero disposti lungo due profili ortogonali, orientati nelle direzioni N-S e E-O. Un'ulteriore stazione sismica è stata installata su un sito di riferimento posto sul bordo orientale del cratere. Un'analisi spettrale preliminare è stata effettuata su alcuni campioni di rumore sismico acquisiti durante l'esperimento.

In futuro, le curve di dispersione delle onde superficiali saranno ottenute utilizzando tecniche di array, come il metodo dell'Autocorrelazione Spaziale (SPAC) di Aki (1957) e le sue recenti modifiche (MSPAC, Bettig et al, 2001; CCA, Cho et al., 2004). Dall'inversione delle curve di dispersione, si otterranno i modelli di velocità per le onde di taglio per i siti campionati da ciascun array. Inoltre la funzione di trasferimento sperimentale sarà calcolata per ogni stazione, usando il metodo di Nakamura e la tecnica dei rapporti spettrali con sito di riferimento.

L'alta densità di stazioni utilizzate nell'esperimento e l'elevato numero di punti campionati permetterà di ottenere una dettagliata struttura crostale e di determinare le frequenze di risonanza e i valori di amplificazione in differenti zone del cratere.

Introduction

The determination of the subsoil structure often requires expensive drilling. An alternative and more economic approach to investigate the shallow velocity structure is based on the analysis of surface waves. In the last years, the determination of the seismic velocities at shallow depths from the dispersion of surface waves has got an increasing popularity and recent results in seismic engineering [Louie, 2001; Bettig et al. 2001] have demonstrated that the inversion of dispersion data can provide very fine resolution of the velocity structure and constrain shallow shear-wave velocities with a minimum level of uncertainty. The multichannel [SPAC, Aki, 1957; MSPAC, Bettig et al., 2001; CCA, Cho et al., 2004] techniques represent a very attractive tool for the phase velocity determination because they can be applied to ambient noise and do not require any artificial energizing source.

The velocity models can be used to evaluate the theoretical ground response to a seismic input [Kramer, 1996]. Such determination is of great relevance especially in densely urbanized areas, where a quantitative assessment of the amplification factors is necessary for a correct evaluation of seismic hazard.

Site transfer function can also be obtained experimentally by using reference- and non-reference-station techniques applied to microtremor. Reference-site techniques use simultaneous recordings from the site of interest and nearby hard-rock site for a direct comparison of ground-motion spectra. Non-reference-site techniques, such as the method of Nakamura [1989], use 3-component signals recorded only at the site of interest and compare the horizontal to vertical (H/V) ground-motion spectra. The maxima of the H/V function, under certain assumptions, correctly indicate the resonance frequencies of soft shallow sediments overlying the bedrock.

The seismic survey carried out at Solfatara

Volcano in the period 2-6 April 2007 is aimed at the detailed determination of the shallow structure and of local site effects. Five seismic arrays were deployed in different areas of the crater in order to sample very local heterogeneities (fig.1). A further seismic station was installed on the eastern rim of the crater.

The recorded microtremor will be analysed by using the Spatial Autocorrelation (SPAC) technique [Aki, 1957] and its modifications, like the Modified Spatial Autocorrelation [MSPAC, Bettig at al., 2001] and the Centerless Circular Array methods [CCA, Cho et al., 2004]. These techniques allow to obtain surface wave dispersion curves that are indicative of the shallow shear-wave velocities. The analyses will be performed for each of the 5 sampled sites, allowing a comparison among the obtained velocity models.

Moreover reference [Borcherdt, 1970] and non-reference [Nakamura, 1989] spectral ratio techniques will be used to estimate at each sampled point the experimental transfer function and hence the resonance frequencies and amplification values.

The obtained results will also be interpreted in terms of some unsolved issues relative to the Solfatara site transfer function, presented in a recent study by Petrosino et al. [2006].

1. Instruments and data

The following instruments were used during the experiment:

5 seismic stations Lennartz MarsLite

5 three-component 1-Hz Mark LE3Dlite seismometers

2 GeoXT Trimble GPS receivers controlled by the TerraSync software

Seismic data were recorded by the seismic stations with a sampling rate of 125 sps and scaling factor of 8μVolt/count. They were stored in binary format on 1GB PC-card DPPCM2 and on 500MB magneto-optical disk. Recorded data were then transferred on PC hard-disk and converted to SAC format (http://www.llnl.gov/sac/).

The most part of the seismometers was buried in approximately 20 cm deep holes. The sensors DR51 and AR52, located near the fumarolic field, and all the geophones of the array B were not buried due to the high temperature reached by the soil in those areas (fig.1). The sen-

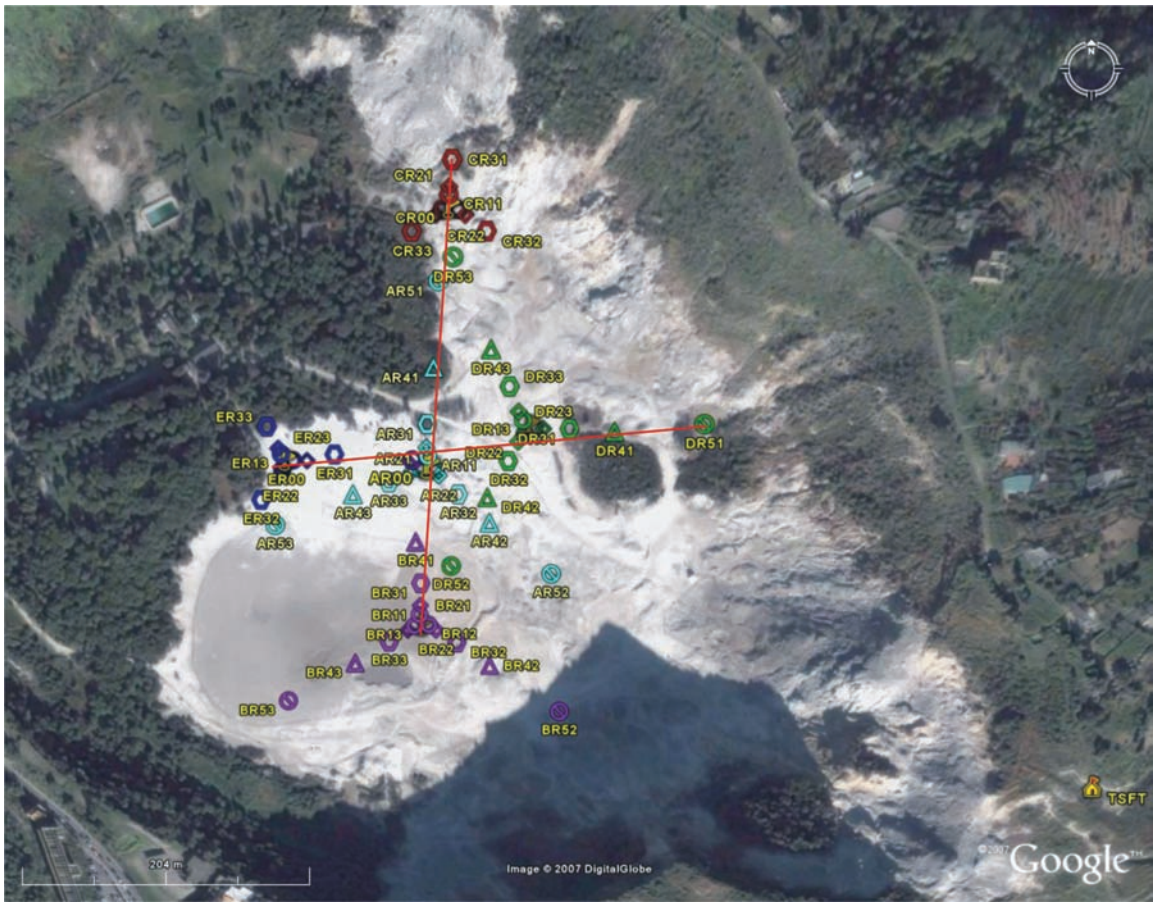

Figure. 1 Array geometry. The red lines indicate the two N-S and E-W oriented profiles.
Figura. 1 Configurazione degli array. Le linee rosse indicano i due profili orientati nelle direzioni N-S e E-O.

Figure 2 Seismic instruments.
Figura 2 Strumentazione sismica utilizzata.

sors were deployed with the horizontal components oriented in the N-S and E-W directions and their coordinates (table 1) were measured using GPS positioning, with a precision of one meter. The power for the instrumental chain was supplied by 12V batteries (fig. 2).

One seismic station (TSFT) was installed on the eastern rim of the crater and set in continuous acquisition mode.

Five circular seismic arrays (A, B, C, D and E) were installed in the Solfatara crater, using the remaining instruments (fig. 1, fig. 3). Each array consisted of 4 sensors, 3 of them evenly spaced (120°) around the circumference and the fourth placed at its center. Arrays A, B and D were designed with radii of 5, 10, 25, 50 and 100 m. Arrays C and E had radii of 5, 10 and 25 m. In fig. 4 the different configurations are shown. Moreover, some stations (fig 1, red lines) of the arrays shaped two orthogonal profiles of about 250-m-length, roughly oriented in the N-S and E-W directions. About 1-hour of seismic noise was recorded for each circular configuration with fixed radius.

The particular geometry of the station deployment was adopted to apply the Spatial Autocorrelation technique [Aki, 1957] and its modifications [Bettig et al., 2001, Cho et al., 2004], to the data recorded by each array and to infer shear-wave velocity models for different areas of the crater. Further information about the shallow structure will come from the application of Nakamura's technique [1989] to microtremor recorded at each sampled site. The two orthogonal profiles oriented N-S and E-W will be useful to map possible variations of the resonance frequencies and amplification values along the N-S and E-W directions.

The level of the local seismic noise will be evaluated comparing the array recordings with those of the reference station TSFT, located outside the crater. This station will also be used as reference station in the application of the spectral ratio technique.

Site name	Latitude N (degree)	Longitude E (degree)	Elevation asl (m)	Radius (m)
AR00	40.828100	14.139419	97	center
AR11	40.828156	14.139420	97	5
AR12	40.828080	14.139470	97	5
AR13	40.828085	14.139362	95	5
AR21	40.828202	14.139411	93	10
AR22	40.828052	14.139492	95	10
AR23	40.828074	14.139296	93	10
AR31	40.828329	14.139424	96	25
AR32	40.827947	14.139628	94	25
AR33	40.828015	14.139130	94	25
AR41	40.828630	14.139482	98	50
AR42	40.827790	14.139851	92	50
AR43	40.827947	14.138865	92	50
AR51	40.829075	14.139532	101	100
AR52	40.827501	14.140298	96	100

AR53	40.827777	14.138286	94	100
BR00	40.827203	14.139341	94	center
BR11	40.827260	14.139314	90	5
BR12	40.827310	14.139326	92	5
BR13	40.827195	14.139273	91	5
BR21	40.827197	14.139384	91	10
BR22	40.827174	14.139438	92	10
BR23	40.827172	14.139226	90	10
BR31	40.827446	14.139335	93	25
BR32	40.827100	14.139592	93	25
BR33	40.827102	14.139085	93	25
BR41	40.827680	14.139307	90	50
BR42	40.826970	14.139836	89	50
BR43	40.826978	14.138821	89	50
BR51	40.828136	14.139306	93	100
BR52	40.826724	14.140357	94	100
BR53	40.826751	14.138300	95	100
CR00	40.829439	14.139626	102	center
CR11	40.829501	14.139624	93	5
CR12	40.829425	14.139683	100	5
CR13	40.829429	14.139575	94	5
CR21	40.829540	14.139626	99	10
CR22	40.829402	14.139730	101	10
CR23	40.829403	14.139530	98	10
CR31	40.829670	14.139651	102	25
CR32	40.829324	14.139876	101	25
CR33	40.829322	14.139363	102	25
DR00	40.828319	14.140157	96	center
DR11	40.828306	14.140191	97	5
DR12	40.828276	14.140115	96	5
DR13	40.828350	14.140106	96	5
DR21	40.828306	14.140250	95	10
DR22	40.828237	14.140069	96	10
DR23	40.828397	14.140076	95	10
DR31	40.828305	14.140440	91	25
DR32	40.828132	14.139998	92	25
DR33	40.828532	14.140015	93	25
DR41	40.828290	14.140758	99	50
DR42	40.827930	14.139839	96	50
DR43	40.828726	14.139889	98	50
DR51	40.828328	14.141383	93	100
DR52	40.827544	14.139560	92	100
DR53	40.829195	14.139637	99	100
ER00	40.828097	14.138410	97	center
ER11	40.828144	14.138456	98	5
ER12	40.828083	14.138367	97	5
ER13	40.828183	14.138367	95	5
ER21	40.828133	14.138550	93	10
ER22	40.828050	14.138350	95	10
ER23	40.828200	14.138350	93	10
ER31	40.828167	14.138750	96	25
ER32	40.827917	14.138200	94	25
ER33	40.828317	14.138283	94	25
TSFT	40.826444	14.144000	175	

Table 1 Coordinates of the sensors.
Tabella 1 Coordinate dei sensori.

Array A configuration

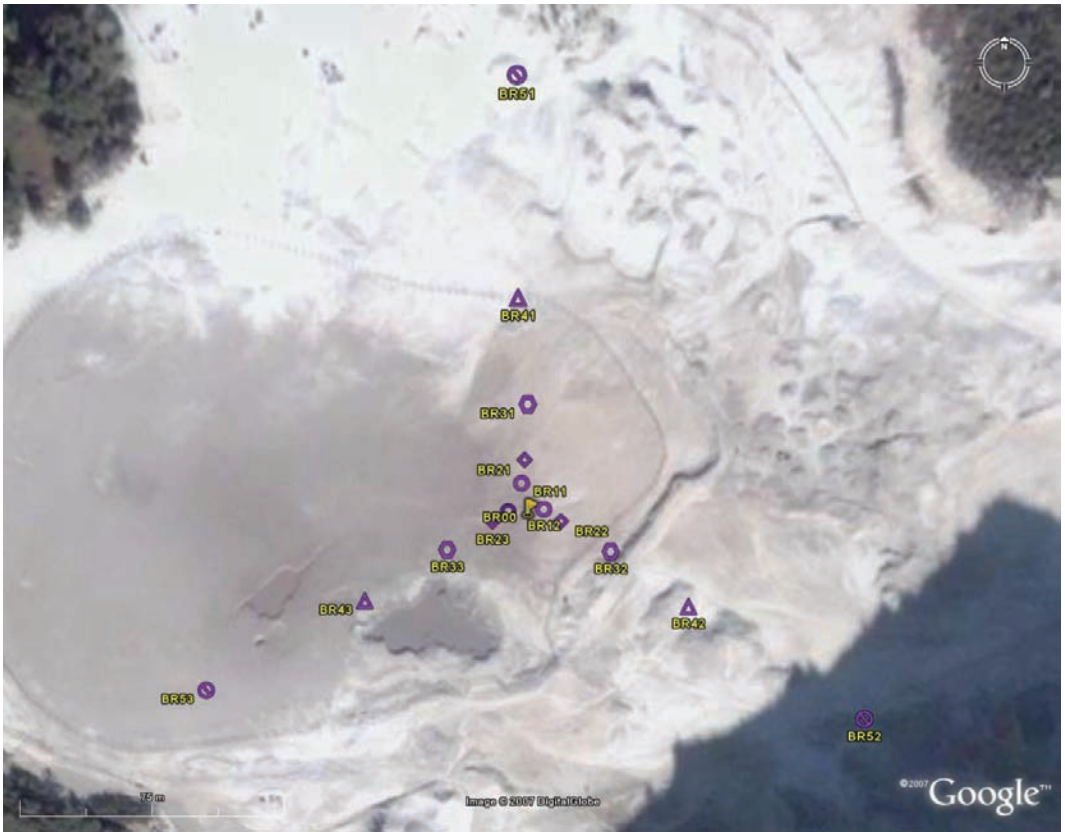

Array B configuration

Array C configuration

Array D configuration

Array E configuration

Figure 3 View of the 5 different configurations of the arrays.
Figura 3 Veduta delle 5 diverse configurazioni degli array.

2. Methodologies

2.1. The Spatial Autocorrelation (SPAC) and Modified Spatial Autocorrelation (MSPAC) technique

The Spatial Autocorrelation method (SPAC) of Aki [1957] allows the estimate of surface wave dispersion curve from multichannel recordings of seismic noise. Under certain assumptions Aki demonstrated that for an array of receivers in a circular configuration around a reference receiver, the phase velocity $c(\omega_0)$ can be obtained by fitting a zeroth-order Bessel function to the azimuthal average of the correlation coefficients $\overline{\rho}(r,\omega_0)$, according to:

$$\overline{\rho}(r,\omega_0) = J_0\left[\frac{\omega_0}{c(\omega_0)}r\right]$$

Extension of Aki's SPAC method to non-circular arrays, known as MSPAC, was proposed by Bettig [2001] and consists in averaging, for each individual target frequency, the correlation coefficients evaluated at subsets of M station pairs whose distances range between *r-dr* and *r+dr*. This procedure allows a robust assessment of the azimuthally averaged correlation coefficients, once the relative position vectors of the selected station pairs depict an uniform and tight sampling of the 0-180° azimuthal range. In this case the condition of having a large number of available inter-station distances can be achieved without the constraint of adopting a particular geometry for the array deployment.

2.2. The Centerless Circular Array technique (CCA)

The Centerless Circular Array (CCA) method for the determination of phase velocity dispersion from microtremor recordings was proposed by Cho et al., [2004]. The technique, initially formulated for centerless circular arrays (fig. 4), was then extended to circular arrays with a central station for the quantification of the signal-to-noise ratio and the estimates of the method's resolution [Cho at al., 2006].

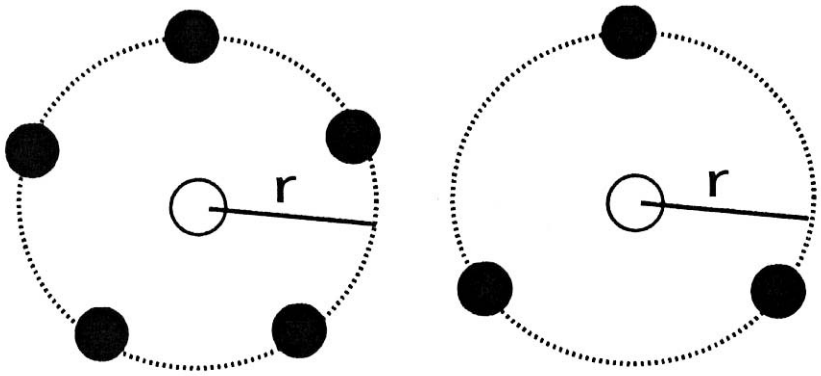

Figure 4 Two possible array configurations for application of the CCA technique.
Figura 4 Due possibili configurazioni di array per l'applicazione del metodo CCA.

If $z(t,r,\theta)$ represents the seismograms available at all the points of the circumference with radius r, two average time histories can be calculated by integrating the signals with different weight functions:

$$\alpha_0(t) = \int_{-\infty}^{\infty} z(t,r,\theta)\,d\theta$$

$$\alpha_1(t) = \int_{-\infty}^{\infty} \exp(-i\theta)\, z(t,r,\theta)\,d\theta$$

It can be demonstrated that the spectral ratio of this two time histories is proportional to the ratio of a zeroth- and first-order Bessel functions and depends only by the product $rk_0(\omega)$ where $k_0(\omega)$ is the wave number:

$$\frac{|\alpha_0(\omega)|^2}{|\alpha_1(\omega)|^2} = \frac{J_0^2[rk_0(\omega)]}{J_1^2[rk_0(\omega)]}$$

Therefore, the phase velocity $c_0(\omega)$ can be estimated from:

$$c_0(\omega) = \frac{r\omega}{F^{-1}\left(|\alpha_0(\omega)|^2 / |\alpha_1(\omega)|^2\right)}$$

where $F^{-1}(\cdot)$ denotes the inverse function.

The advantage of the CCA technique is that accurate and stable phase velocity estimates can be obtained even with a minimum number of sensors.

2.3. The horizontal to vertical spectral ratio technique

The idea that the horizontal to vertical (H/V) spectral ratio of microtremor was representative of the site transfer function was initially proposed by Nogoshi and Igarashi [1971]. These authors justified their assumption suggesting that the observed peak of the H/V ratio was related to the ellipticity curve of fundamental mode Rayleigh waves and it was indicative of the shallow soil structure. In 1989 Nakamura revisited the method proposing a new semi-qualitative theoretical explanation in terms of multiple refractions of SH waves. He claimed that the peak in the H/V spectral ratio is due to vertical incident SH wave, therefore it represents a reliable estimate for the site transfer function of the S waves. According to this interpretation, the site amplification can be calculated as:

$$S_j(f) = \frac{H_j(f)}{V_j(f)}$$

Sj = amplification at the j-th site
Hj = horizontal component spectral amplitude at the j-th site
Vj = vertical component spectral amplitude at the j-th site

Many authors have proved the validity of the technique in the prediction of the resonance frequency with empirical and numerical results [Lermo and Chavez-Garcia, 1994; Castro et al., 1997]. However some authors [Luzon et al., 2001; Malischewsky and Scherbaum, 2004] have found that in the case of low impedance contrast, the method does not predict accurately the resonance frequencies and the amplification levels.

2.4. The reference-site spectral ratio technique

The transfer function is obtained by estimating the spectral ratio of the vertical compo-

nent of motion recorded simultaneously at the site of interest and at a reference site (generally chosen on hard-rock) with negligible amplification [Borcherdt, 1970]. The amplification S^{SR}_j at the j-th site respect to the reference site is expressed as:

$$\ln S_j^{SR}(f) = \ln A_j(f) - \ln A_R(f)$$

A_R = average spectral amplitude at the reference site
A_j = average spectral amplitude at the j-th site

This technique is considered the most reliable in the determination of either the amplification and resonance frequency of the site.

3. Data analysis

In the following we report some examples of spectral analysis performed on about 1-hour of microtremor recorded by the central stations of each array and for the reference station TSFT.

The spectra evidence some high frequency noise (> 10 Hz) due to the presence of the numerous tourists walking in the field. Moreover, recordings of the array B are affected by a low frequency peak (< 1 Hz) due to the strong wind occurred during that day, and a high frequency peak at about 28 Hz probably due to the wind-induced vibrations of some nearby objects. Seismic noise recorded by the station TSFT, which thanks to its position was not affected by the noise produced by nearby walking people, is characterized by a lower spectral content, mainly comprised in the 1-10 Hz frequency range.

Spectral analysis was repeated after filtering the seismograms below 10 Hz, to further investigate the spectral properties in the frequency range that will be used for the seismological analysis. The filtered signals recorded at the station AR00 (fig. 5), installed approximately at the center of the crater, show a spectral peak on the vertical component at about 8 Hz and a maximum at about 5 Hz on the horizontal components. The same pattern is observed at the station BR00 (fig. 6), located in the area of the mud-pool. The station CR00, located in the northern area, shows a slightly higher frequency content, being the main spectral peak on the vertical component at 10 Hz, while peaks on the horizontal components appear between 5 and 10 Hz (fig. 7). In the eastern part, near the fumarolic field, spectral peaks at 2 and 8 Hz are observed in the seismic noise recorded by the station DR00 (fig. 8). Finally the station ER00, located at the West, shows amplitude peaks spread in the 5-10 Hz band (fig. 9). The spectral content of the 10-Hz-low-pass filtered microtremor recorded at the stations located in the crater are quite different from those observed at the reference station TSFT, installed on the eastern rim. Actually, TSTF spectra evidence a lower frequency content, with main peaks at a 2.5 and 1 Hz (fig. 10).

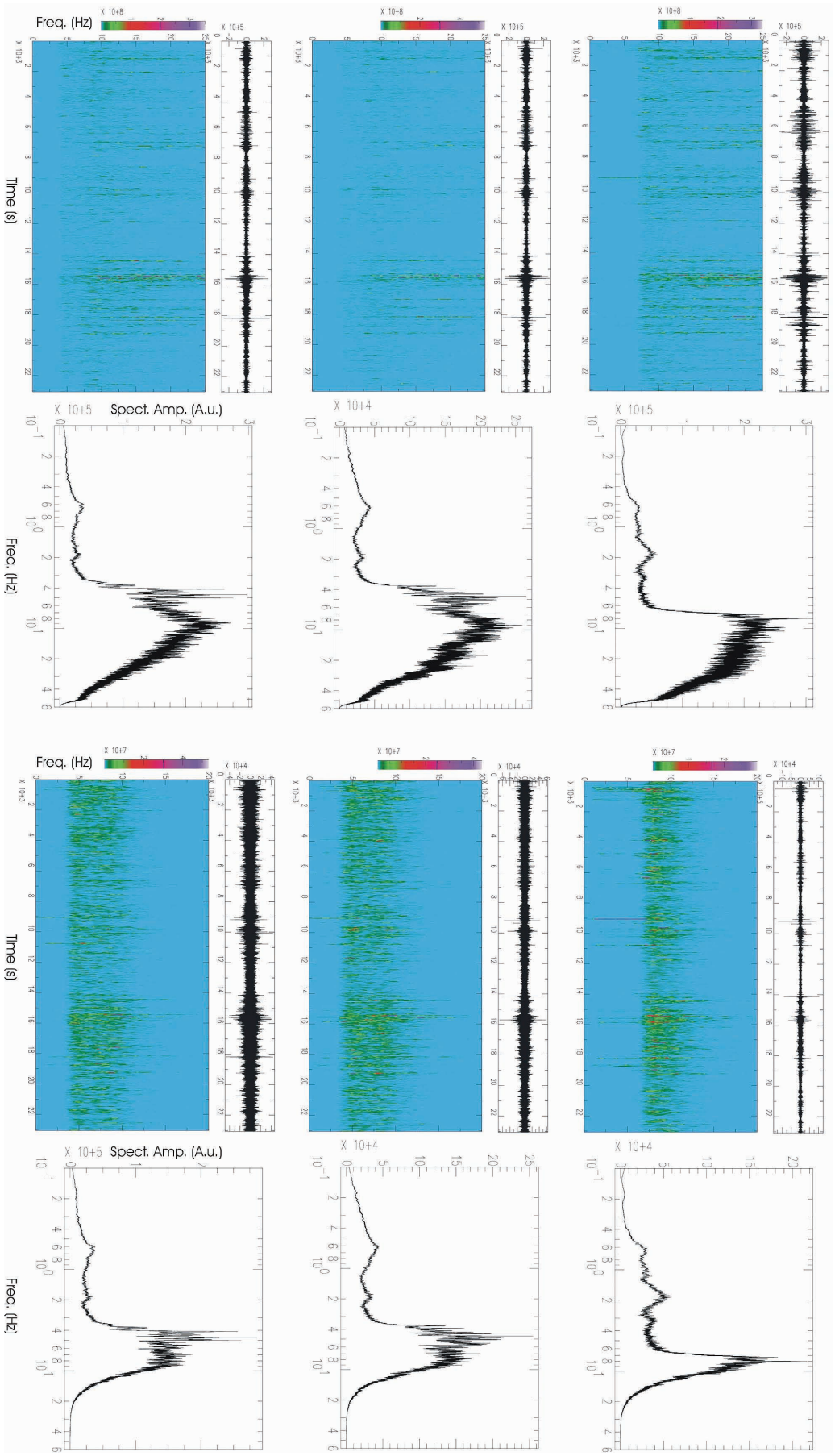

Figure 5 Spectral analysis of the seismic noise recorded by station AR00. From the top to the bottom: vertical, N-S and E-W component. From the left to the right: unfiltered spectrogram, unfiltered spectrum, filtered spectrogram and filtered spectrum.

Figura 5 Analisi spettrale del rumore sismico registrato dalle stazione AR00. Dall'alto verso il basso sono riportate le componenti verticali, N-S e E-O del segnale. Da sinistra verso destra si riporta lo spettrogramma non filtrato, lo spettro non filtrato, lo spettrogramma filtrato e lo spettro filtrato.

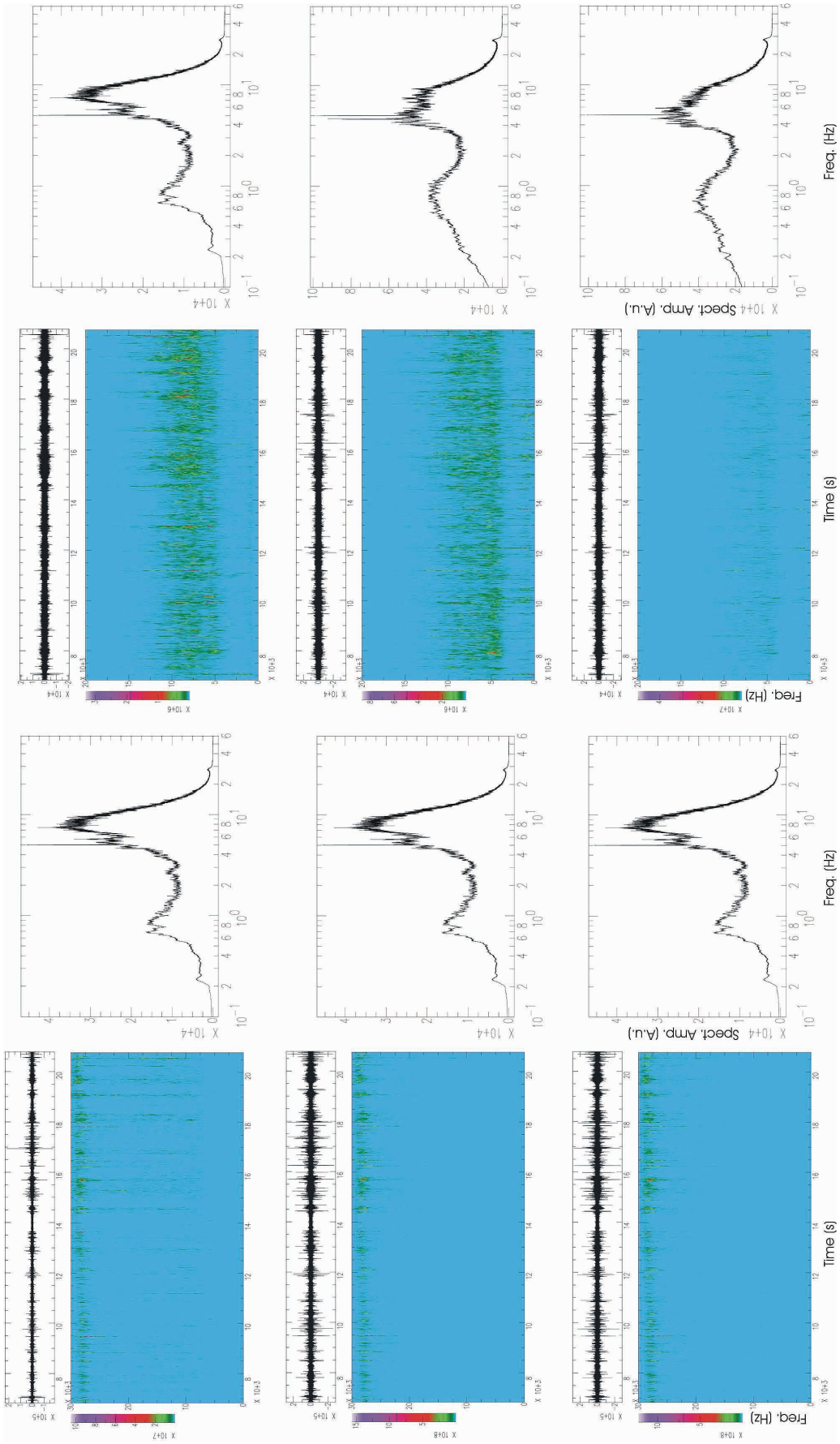

Figure 6 Spectral analysis of the seismic noise recorded by station BR00. From the top to the bottom: vertical, N-S and E-W component. From the left to the right: unfiltered spectrogram, unfiltered spectrum, filtered spectrogram and filtered spectrum.
Figura 6 Analisi spettrale del rumore sismico registrato dalle stazione BR00. Dall'alto verso il basso sono riportate le componenti verticali, N-S e E-O del segnale. Da sinistra verso destra si riporta lo spettrogramma non filtrato, lo spettro non filtrato, lo spettrogramma filtrato e lo spettro filtrato.

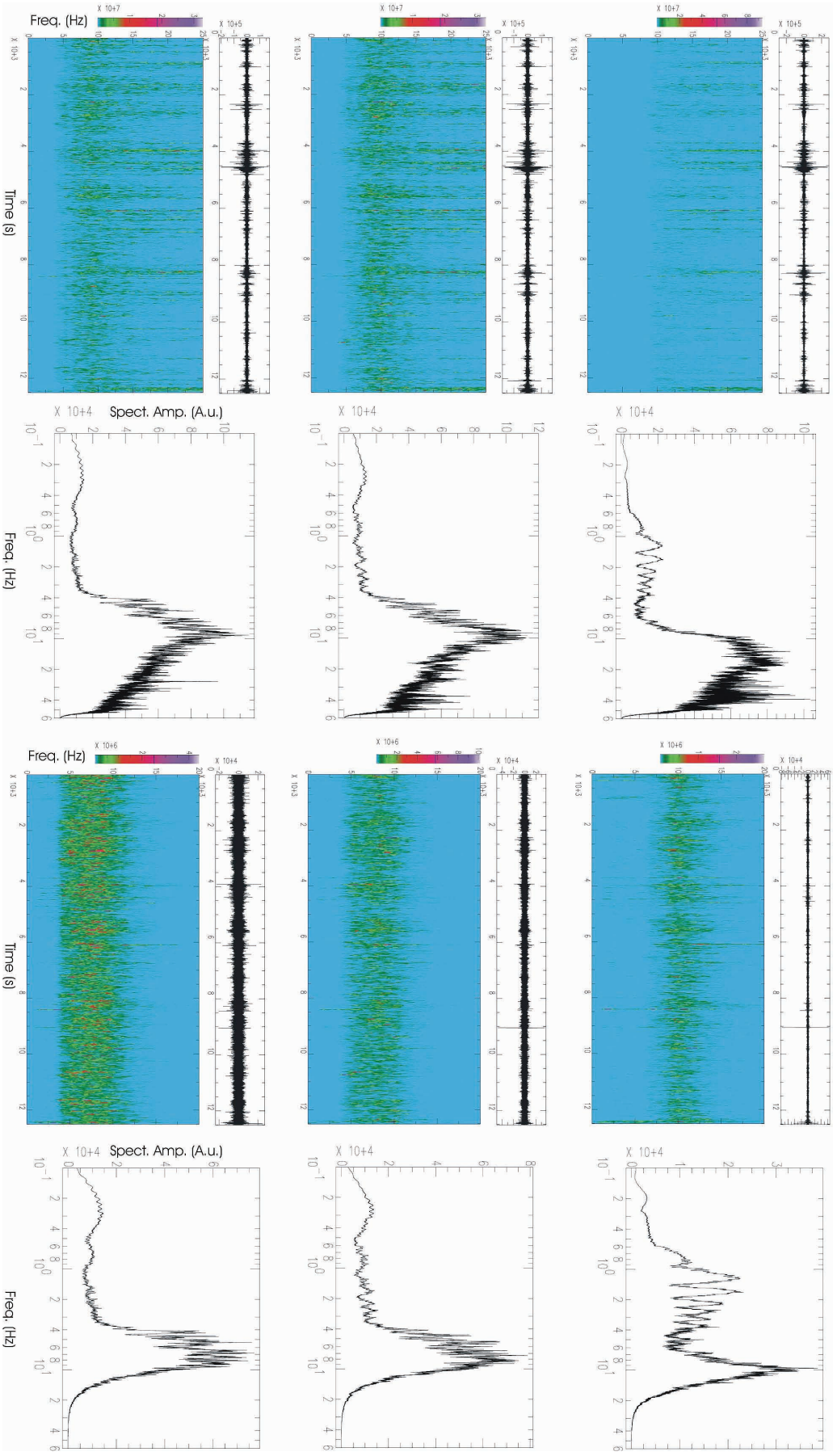

Figure 7 Spectral analysis of the seismic noise recorded by station CR00. From the top to the bottom: vertical, N-S and E-W component. From the left to the right: unfiltered spectrogram, unfiltered spectrum, filtered spectrogram and filtered spectrum.

Figure 7 Analisi spettrale del rumore sismico registrato dalle stazione CR00. Dall'alto verso il basso sono riportate le componenti verticali, N-S e E-O del segnale. Da sinistra verso destra si riporta lo spettrogramma non filtrato, lo spettro non filtrato, lo spettrogramma filtrato e lo spettro filtrato.

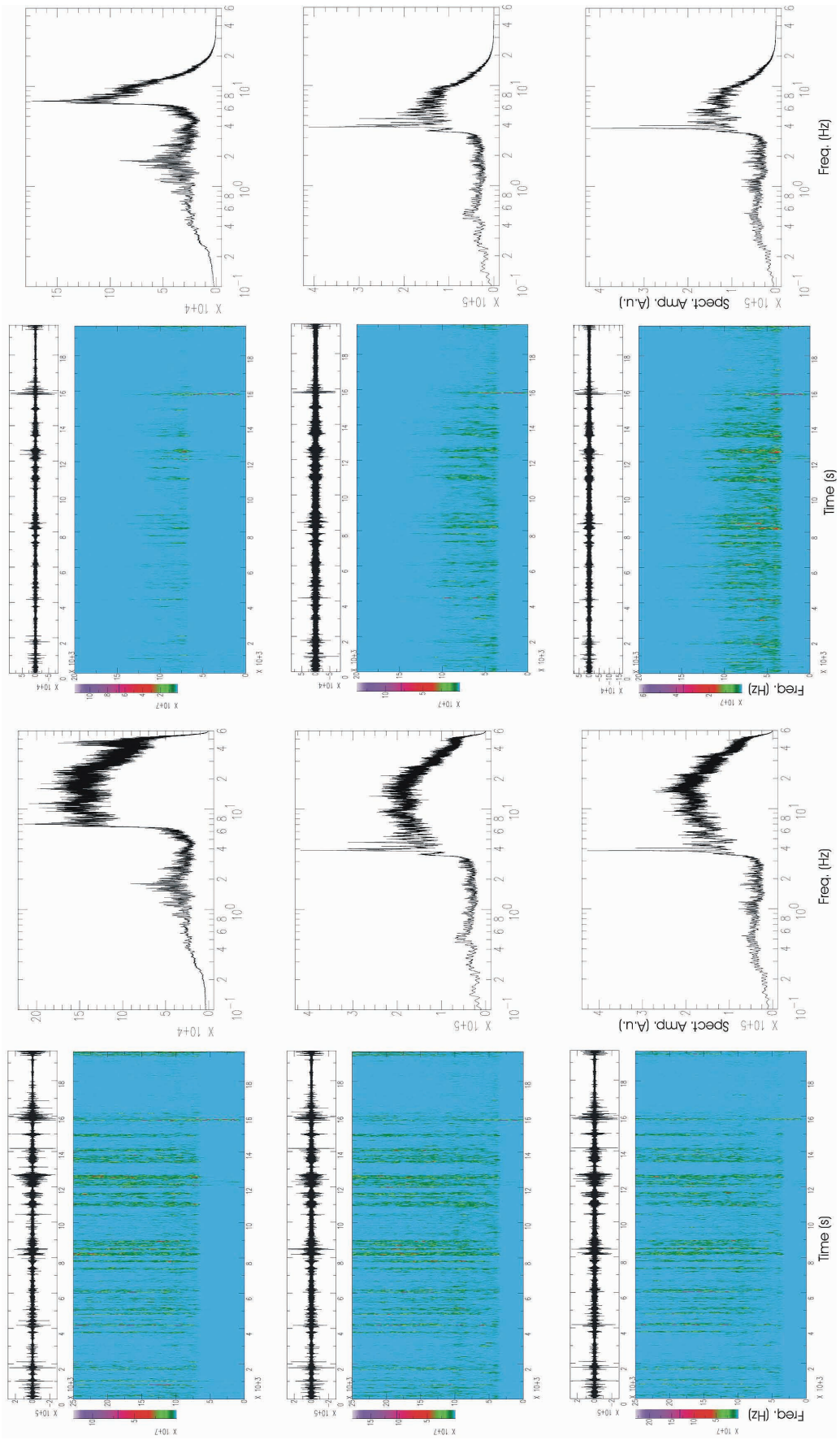

Figure 8 Spectral analysis of the seismic noise recorded by station DR00. From the top to the bottom: vertical, N-S and E-W component. From the left to the right: unfiltered spectrogram, unfiltered spectrum, filtered spectrogram and filtered spectrum.
Figura 8 Analisi spettrale del rumore sismico registrato dalle stazione DR00. Dall'alto verso il basso sono riportate le componenti verticali, N-S e E-O del segnale. Da sinistra verso destra si riporta lo spettrogramma non filtrato, lo spettro non filtrato, lo spettrogramma filtrato e lo spettro filtrato.

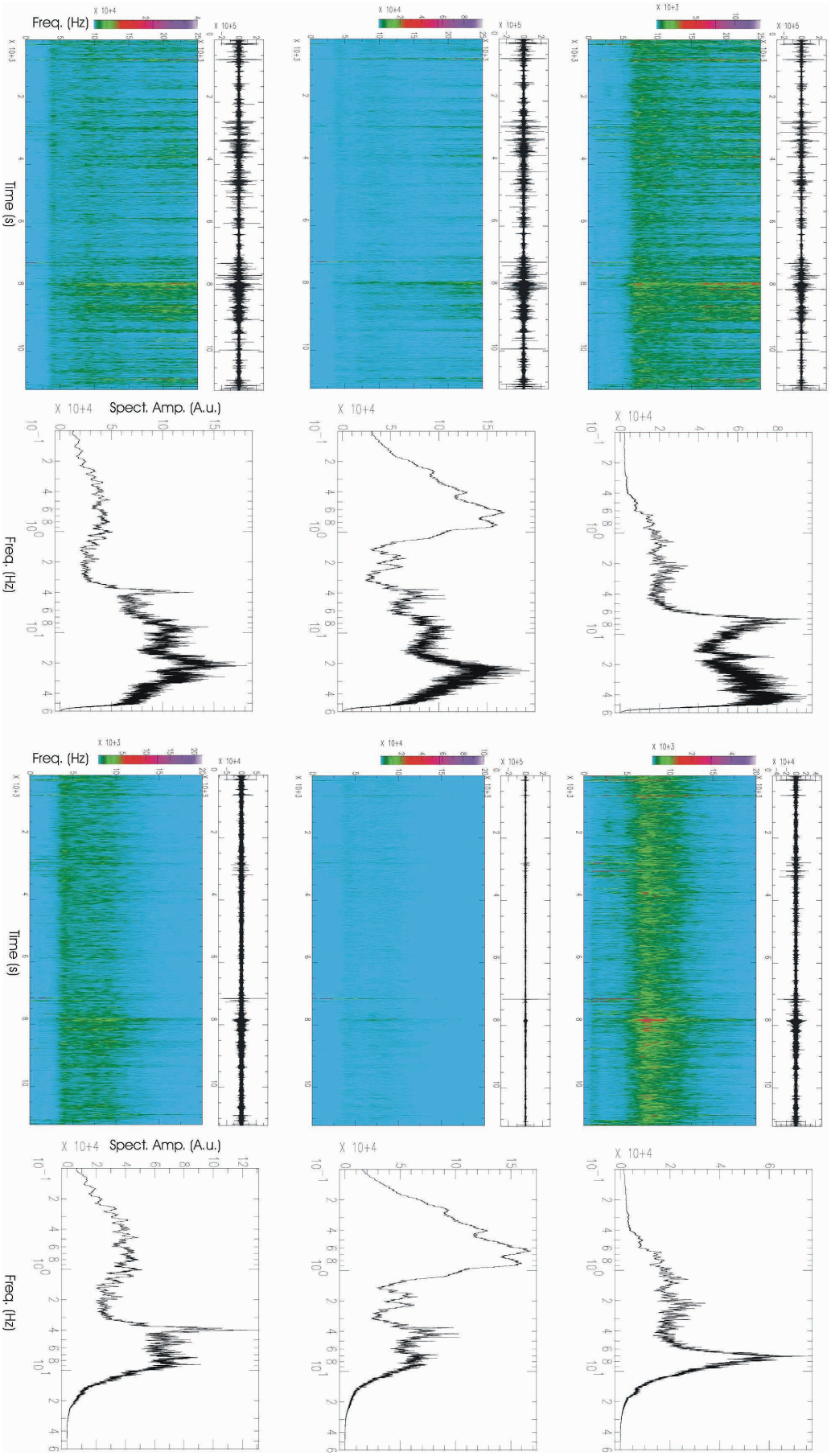

Figure 9 Spectral analysis of the seismic noise recorded by station ER00. From the top to the bottom: vertical, N-S and E-W component. From the left to the right: unfiltered spectrogram, unfiltered spectrum, filtered spectrogram and filtered spectrum.

Figura 9 Analisi spettrale del rumore sismico registrato dalle stazione ER00. Dall'alto verso il basso sono riportate le componenti verticali, N-S e E-O del segnale. Da sinistra verso destra si riporta lo spettrogramma non filtrato, lo spettro non filtrato, lo spettrogramma filtrato e lo spettro filtrato.

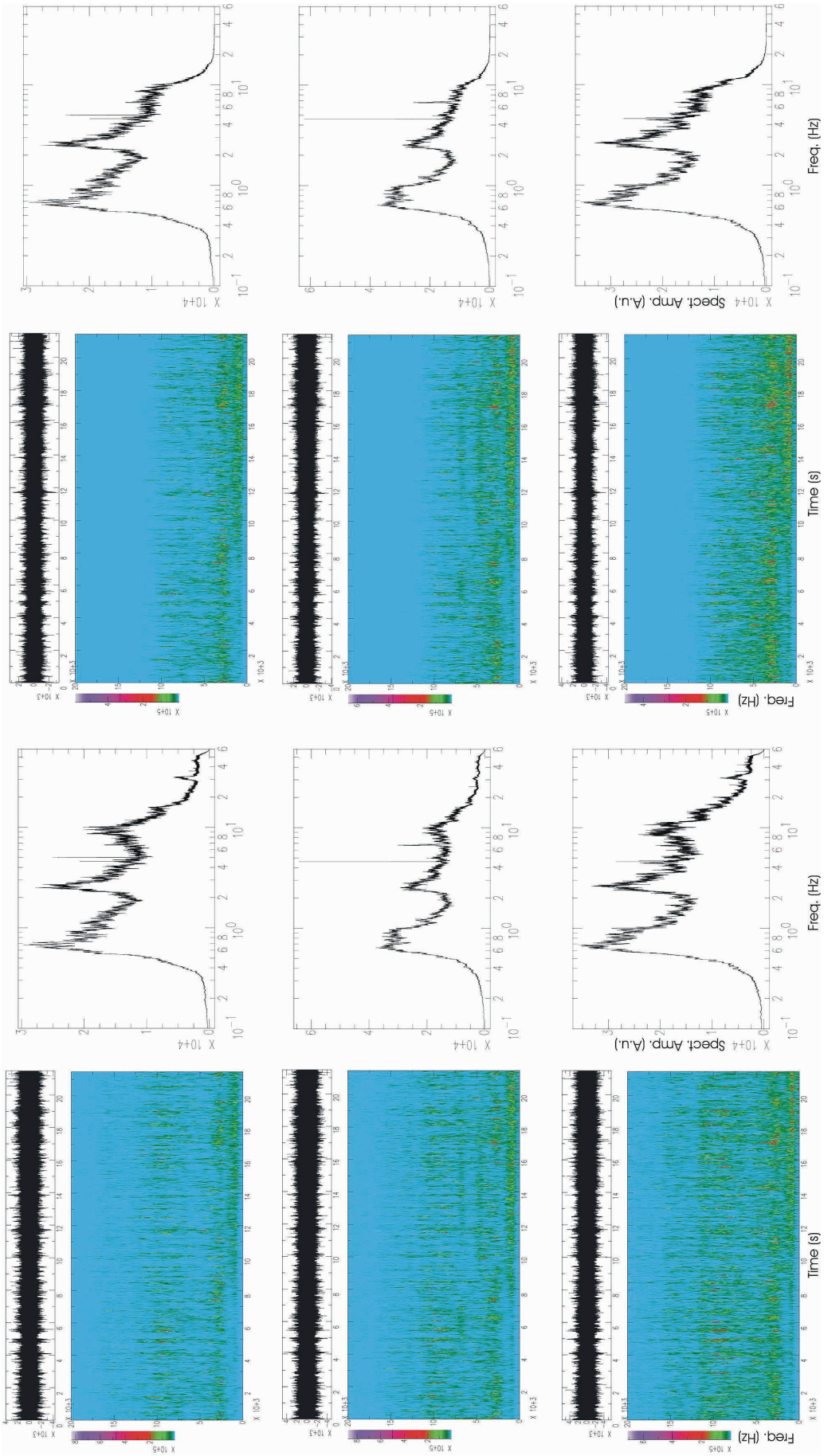

Figure 10 Spectral analysis of the seismic noise recorded by station TSFT. From the top to the bottom: vertical, N-S and E-W component. From the left to the right: unfiltered spectrogram, unfiltered spectrum, filtered spectrogram and filtered spectrum.
Figura 10 Analisi spettrale del rumore sismico registrato dalle stazione TSFT. Dall'alto verso il basso sono riportate le componenti verticali, N-S e E-O del segnale. Da sinistra verso destra si riporta lo spettrogramma non filtrato, lo spettro non filtrato, lo spettrogramma filtrato e lo spettro filtrato.

Conclusions

The results of the preliminary spectral analysis of some samples of seismic noise recorded during the 2-6 April 2007 survey at Solfatara Volcano, suggest to get more insights in the wavefield properties in order to exclude external disturbances due both to the antropic activity and to the unfavourable weather condition. However, these first results are already indicative of differences among the spectral content of the microtremor recorded in different areas of the crater. In particular the most evident differences are observed between the recordings of the stations located in the central part of the crater and those deployed in the northern and eastern areas. Moreover, the seismic noise recorded outside the crater by the station TSFT has spectral characteristics that are very different from those observed for the array stations.

The observed differences in the spectral content of the seismic noise could be due both to the presence of horizontal velocity contrasts and to variations of the thickness of the shallower layers.

As future development, both array and single station techniques will be applied to the recorded data-set in order to better define the crustal structure of the volcano, to investigate about the presence (or not) of lateral heterogeneities, and to estimate local site effects.

Acknowledgments

The Administration of Solfatara Volcano is fully acknowledged for having allowed us to deploy the seismic instruments in the Naturalistic Park.

References

Aki, K., (1957). *Space and time of stationary stochastic wave, with special reference to microtremors*. Bull. Earthq. Res. Ins., XXXV, 415-457.

Bettig, B., Bard, P.Y., Scherbaum, F., Riepl, J., Cotton, F., Cornou, C. and Hatzfeld, D., (2001). *Analysis of dense array noise measurements using the modified spatial auto-correlation method (SPAC). Application to the Grenoble area*. Bollettino di Geofisica Teorica ed Applicata, 42, 281-304.

Borcherdt, R.D., (1970). *Effects of local geology on ground motion near San Francisco Bay*. Bull. Seis. Soc. Am, 60, 29-61.

Castro, R., Mucciarelli, M., Pacor, F., Petrungaro, C., (1997). *S-wave site respons estimates using horizontal to vertical spectral ratios*. Bull. Seism. Soc. Am., 87, no. 1, 256–260.

Cho I., T. Tada and Y. Shinozaki (2004). A new method to determine phase velocities of Rayleigh waves from microseisms. Geophys., 69, NO. 6, 1535-1551.

Cho, I., Tada, T. and Shinozaki, Y., (2006). *Centerless circular array method: Inferring phase velocities of Rayleigh waves in broad wavelength ranges using microtremor records.* J. Geophy. Res., 111, N. B09315, doi:10.1029/2005JB004235.

Kramer, S.L., (1996). *Geotechnical earthquake engineering*. Prentice Hall Inc., Upper Saddle River, New Jersey.

Lermo, J. and Chavez-Garcia, F. J., (1994). *Are microtremors useful in site response evaluation?*. Bull. Seism. Soc. Am., 84, 1350–1364.

Louie, J. N., (2001). *Faster, better: Shear–wave velocity to 100 meters depth from refraction microtremor arrays*. Bull. Seism. Soc. Am., 91, 347-364.

Luzon, F., Al Yuncha, Z., Sanchez-Sesma, F.J. and Ortiz-Aleman, C., (2001). *A Numerical Experiment on the Horizontal to Vertical Spectral Ratio in Flat Sedimentary Basins.* Pure Appl. Geophys., 158, 2451-2461

Malischewsky, P.G. and Scherbaum, F., (2004). *Love's formula and H/V-ratio (ellipticity) of Rayleigh waves*. Wave Motion, 40, 57-67.

Nakamura, Y., (1989). *A method for dynamic characteristics estimation of subsurface using microtremor on the ground surface*. Quarterly Report of Railway Technical Research Institute (RTRI), Vol. 30, No. 1.

Nogoshi, M. and Igarashi, T., (1971). *On the Amplitude Characteristics of Microtremor (Part 2)* (in Japanese with English abstract). Jour. Seism. Soc. Japan, 24, 26-40.

Petrosino, S., Cusano, P. and Saccorotti, G., (2006). *Shallow shear-wave velocity structure of Solfatara volcano (Campi Flegrei, Italy), from inversion of Rayleigh-wave dispersion curves*. Bull. Geof. Teo. Appli., 47, n. 1-2, pp. 89-103.

Istituto Nazionale di Geofisica e Vulcanologia
Via di Vigna Murata, 605 - 00143 Roma - Italy
www.ingv.it